Markov Modeling of Minimally Invasive Surgery Based on Tool/Tissue Interaction and Force/Torque Signatures for Evaluating Surgical Skills

Jacob Rosen, Blake Hannaford*, *Member, IEEE*, Christina G. Richards, and Mika N. Sinanan

***Abstract*—The best method of training for laparoscopic surgical skills is controversial. Some advocate observation in the operating room, while others promote animal and simulated models or a combination of surgery-related tasks. A crucial process in surgical education is to evaluate the level of surgical skills. For laparoscopic surgery, skill evaluation is traditionally performed subjectively by experts grading a video of a procedure performed by a student. By its nature, this process uses fuzzy criteria. The objective of the current study was to develop and assess a skill scale using Markov models (MMs). Ten surgeons [five novice surgeons (NS); five expert surgeons (ES)] performed a cholecystectomy and Nissen fundoplication in a porcine model. An instrumented laparoscopic grasper equipped with a three-axis force/torque (F/T) sensor was used to measure the forces/torques at the hand/tool interface synchronized with a video of the tool operative maneuvers. A synthesis of frame-by-frame video analysis and a vector quantization algorithm, allowed to define F/T signatures associated with 14 different types of tool/tissue interactions. The magnitude of F/T applied by NS and ES were significantly different ($p < 0.05$) and varied based on the task being performed. High F/T magnitudes were applied by NS compared with ES while performing tissue manipulation and vise versa in tasks involved tissue dissection. From each step of the surgical procedures, two MMs were developed representing the performance of three surgeons out of the five in the ES and NS groups. The data obtained by the remaining two surgeons in each group were used for evaluating the performance scale. The final result was a surgical performance index which represented a ratio of statistical similarity between the examined surgeon's MM and the MM of NS and ES. The difference between the performance index value, for a surgeon under study, and the NS/ES boundary, indicated the level of expertise in the surgeon's own group. Using this index, 87.5% of the surgical procedures were correctly classified into the NS and ES groups. The 12.5% of the procedures that were misclassified were performed by the ES and classified as NS. However in these cases the performance index values were very close to the NS/ES boundary. Preliminary data suggest that a performance index based on MM and F/T signatures provides an objective means of distinguishing NS from ES. In addition, this methodology can be further applied to evaluate haptic virtual reality surgical simulators for improving realism in surgical education.**

Manuscript received February 18, 2000; revised January 13, 2001. This work was supported by the U.S. Army Medical Research and Material Command under DARPA Grant DMAD17-97-1-725, and by a major grant from US Surgical, a division of Tyco, Inc. to the University of Washington, Center for Videoendoscopic Surgery. *Asterisk indicates corresponding author.*

J. Rosen is with the Department of Electrical Engineering, University of Washington, Seattle, WA 98195 USA (rosen@u.washington.edu).

*B. Hannaford is with the Department of Electrical Engineering, Box 352500, University of Washington, Seattle, WA 98195 USA (e-mail: blake@u.washington.edu).

C. Richards and M. Sinanan are with the Department of Surgery, University of Washington, Seattle, WA 98195 USA.

Publisher Item Identifier S 0018-9294(01)03397-3.

***Index Terms*—Endoscopy, haptics, hidden Markov model, human machine interface, minimally invasive surgery (MIS), soft tissues, surgical simulation, surgical training.**

I. Introduction

THE USE OF minimally invasive surgical (MIS) techniques has become widespread only within the last ten years. Although the technology has been available in some form for over 100 years, only recently has the instrumentation developed to an extent that makes the performance of laparoscopic general surgical procedures possible. Using a miniature video camera and instruments inserted through small portals, operations previously performed through large incisions that required long recovery times are now performed with a much shorter recovery. The use of this new technology has also presented a new set of problems; namely, the training of individuals to perform techniques that require a new set of skills. One of the more difficult tasks in surgical education is to teach the optimal application of instrument forces and torques necessary to conduct an operation. This is especially problematic in the field of MIS where the teacher is one step removed from the actual conduct of the operation.

Surgical skills of MIS performed by senior surgeons and surgeons during their residency were evaluated objectively by using mechanical models, animal models and virtual reality (VR) simulators with or without haptic interface. The surgical tasks used for skill evaluation have varied from simple actions like peg transfers, pattern cutting, clip and divide, endolooping, mesh placement, fixation [1], drilling [2], transferring small inanimate objects [5], making multiple defined incisions [6], suturing with intracorporeal or extracorporeal knots [1]–[5], [7], [8], and palpation [9], [10] to full surgical procedure [8], [11]. The quantitative parameters for skill evaluation in these tasks were in some cases only single measures such as completion time, and other multiple parameter indexes, virtual position, virtual force, and a checklist.

The development of a surgical simulation system to achieve the goals of safe and adequate training in a cost-effective manner is a very real necessity. Such a system holds promise for providing a less stressful learning environment for the surgical student while eliminating risks to the patient. It would permit training outside of the operating room and could also support a measurement of competence—much akin to a pilot training in a flight simulator. The use of VR models for teaching these complex surgical skills has been a long-term goal of

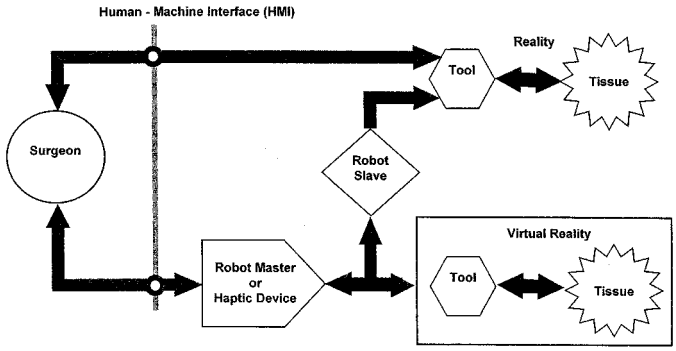

Fig. 1. The human machine interface in several surgical systems setups—General overview.

numerous investigators [14]–[16]. Many of these simulators under development couple the VR computer graphics with haptic (F/T reaction) feedback devices in order to provide a fully immersed virtual environment, combining both visual and haptic feedback of the tool/tissue interaction during the surgical procedures [7], [11], [13], [17]–[19]. In parallel to the VR in medical training stations, the use of robotic technology to aid surgeons has been actively studied [20]–[26]. Commercial surgical robotic systems, like ZEUS by Computer Motion and the daVinci system by Intuitive Surgical, Inc., which are still in clinical trials, may redefining the operating room of the future.

What both MIS, the VR/haptic surgical training stations, and surgical robots have in common is a new human/machine interface (HMI)—Fig. 1. This HMI may be subdivided into human/tool and tool/tissue interfaces. While other studies have focused on the tool-tip/tissue interaction [10], [27], [28], our research is aimed at analyzing the human/tool interface in MIS.

The methodology developed in the current study was based on Markov modeling (MM) and a subset of hidden Markov modeling (HMM). HMM were extensively developed in the area of speech recognition [29], [32]–[34]. Based on the theory developed for speech recognition HMMs were emerged in the field of human operator modeling in general, and robotics in particular. HMMs were applied for studying teleoperation [35]–[37], human manipulation actions [38], human skills evaluation for the purpose of transferring human skill to robots [39]–[41], and manufacturing applications [42], [43]. Gesture recognition with HMMs has also received increasing recent attention from the rehabilitation technology community (see [44] for review). They are also being applied to the recognition of facial expressions from video images [45]. Moreover, HMMs may well prove useful in many of the other emerging applications beyond human computer interfaces, e.g., DNA and Protein modeling [46], fault diagnosis in nuclear power plants [47], and detection of pulsar signals [48]. Clearly, there is a flowering of research in the last few years in this area indicating a wide appreciation of the potential of HMMs to provide better models of the human operator in complex interactive tasks with machines.

The goal of this study was to create new quantitative knowledge of the forces and torques applied by the surgeons on their instruments during minimally invasive surgery. This goal was pursued through several objectives: 1) developing a modified surgical grasper containing embedded sensors that were capable of measuring the forces and torques (F/T) applied by the surgeons during *in-vivo* MIS; 2) creating a database of F/T signals during actual operating conditions on experimental animals; and 3) developing statistical models (MMs) of the F/T data, which can be used to characterize surgical skills. Statistical models of this database can be used to objectively evaluate surgical skills for training advanced laparoscopic surgical procedures and verifying surgical training systems in addition to optimizing designs for surgical simulators and robots.

II. Materials and Methods

A. Experimental System Setup

The experimental setup, shown schematically on Fig. 2(a) includes two sources of information which were acquired while performing the MIS procedures: 1) F/T data measured at the human/tool interface and 2) visual information of the tool tip interacting with the tissues. The two sources of information were synchronized in time and recorded simultaneously for off-line analysis.

The forces and torques at the interface between the surgeon's hand and the endoscopic grasper handle were measured by two sensors. The first sensor was a three-axis F/T sensor (modified ATI—Mini model) which was mounted into the outer tube (proximal end) of a standard reusable 10-mm endoscopic grasper (Karl Storz)—Fig. 3(a). The sensor was capable of simultaneously measuring three components of force (F_x, F_y, F_z) and three components of torque (T_x, T_y, T_z) in the Cartesian frame [Fig. 3(b)]. The sensor orientation was such that X and Z axes generated a plane that was parallel to the end effector's internal contact surface when closed, and the Y and Z axes defined a plane which was perpendicular to this surface.

The second force sensor (Futek—FR1010) was mounted on the endoscopic grasper handle measuring the forces applied by the surgeon's thumb on the grasper's handle. Due to the sensor's two beam parallel structure, it measured only the force component that was perpendicular to the handle. This force component (F_g) generates the moment on the handle which in turn creates the grasping/spreading interactions between the tissue and the tool tip.

The seven channels of F/T data ($F_x, F_y, F_z, T_x, T_y, T_z, F_g$) were sampled at 30 Hz using a laptop computer with a PCMCIA 12 bit A/D card (National Instruments—DAQCard 1200). Preliminary measurements at 1 kHz showed that 99% of the F/T signals' energy (PSD) was included in the 0–10 Hz bandwidth. In addition to the data acquisition, a LabView (National Instruments) application was developed incorporating a graphical user interface for visualizing the F/T data in real-time superimposed with the view from the endoscopic camera monitoring the movement of the grasper while interacting with the internal tissues and organs [Fig. 2(b)]. This synchronized visual integration was achieved by using a video mixer in a picture-in- picture mode. The integrated interface was recorded during the surgical operation for off-line analysis.

One of the grasper's mechanical features enabled the surgeon to rotate the grasper's outer tube, using a joint located near the handle, in order to change the orientation of the tool

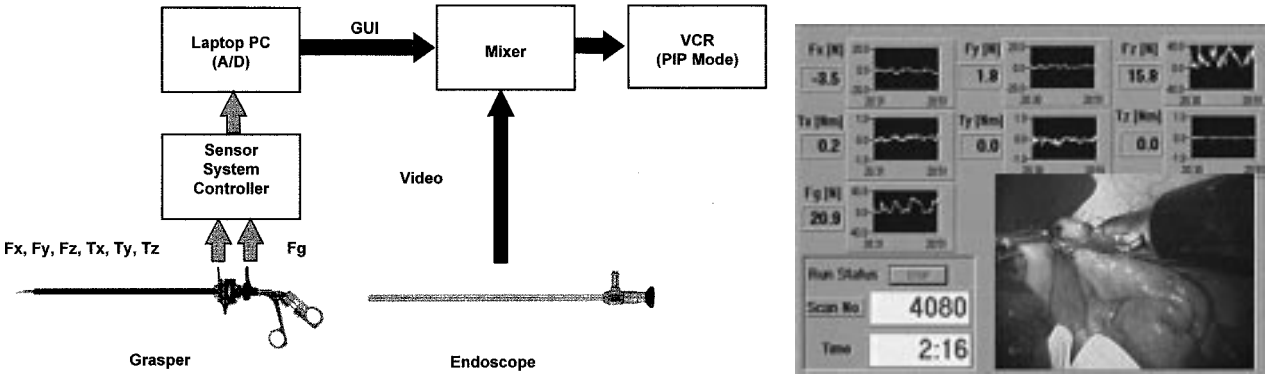

Fig. 2. Experimental setup: (a) Block diagram of the experimental setup integrating the F/T data and the view from the endoscopic camera, (b) Real-Time user interface of F/T information synchronized with the endoscopic view of the procedure using picture-in-picture mode.

tip relative to the grasped tissue without changing the handle orientation. The alignment between the tool tip origin and the sensor remained unchanged since the outer tube and the tool tip were linked mechanically. Moreover, due to the grasper's internal mechanism and the location of the F/T sensor, whenever a grasping force was applied to the handle (F_g), the grasper's outer tube was compressed. This tube compression was sensed by the F/T sensor (F_z). The internal force coupling was defined by a transfer function in the frequency domain, evaluated based on preliminary measurement (Kinematic analysis of this mechanism was performed in [10]). This transfer function was further used to decouple the force measurements included in the database.

B. Surgical Experiment Setup and Clinical Trial Protocol

Ten surgeons [five novice surgeons (NS) and five experienced surgeons (ES)] participated in the experiment following a clinical protocol that included three major steps. During the first step each one of the subjects watched a video of the surgical procedures guided by an experienced surgeon. In the second step, each one of the subjects performed a laparoscopic cholecystectomy and laparoscopic Nissen fundoplication in a porcine model (pig). During the third step all the subjects performed each one of the 14 different pre-defined tool movements (Table II) in a repeatable fashion for one minute while interacting with the same organs and soft tissues as in the surgical procedures. During these interactions the typical F/T involved in manipulating and dissecting the soft tissue were recorded.

In laparoscopic cholecystectomy, the gallbladder is removed due to pain and inflammation from gallstone, whereas laparoscopic Nissen Fundoplication is performed to correct gastroesophageal reflux. Each operation was divided into steps (Table I). Although all the steps were performed for each procedure, data were recorded only when the instrumented grasper was used with the following tool tips: atraumatic grasper, curved dissector, and Babcock grasper [Fig. 3(c)]. During the surgical procedure, the endoscopic camera was held by the same experienced surgeon who also served as an assistant throughout the whole surgery. A template was used for determining the port location of the tools and the camera. All the surgical procedures were performed by the ten surgeons using the same tools, port locations, and approximately the same animal size. Protocols for anesthetic management, euthanasia, and survival procedures were reviewed and approved by the Animal Care Committee of the University of Washington and the Animal Use Review Division of the U.S. Army Veterinary Corps.

C. Data Analysis

Three types of analysis were performed on the raw data: 1) video analysis (VA) encoding the type of tool-tip/tissue interaction; 2) vector quantization (VQ) encoding the F/T data into clusters (signatures); and 3) Markov modeling (MM) for evaluating surgical skill level. Using the human language as an analogy, the VA was performed by an expert surgeon to identify the basic "*words*" of the MIS "*language*" for creating a "*dictionary*." In the same way as a single word is pronounced differently by different people, the same tool/tissue interaction is performed differently by different surgeons, yet they all share the same meaning, or outcome, as in the realm of surgery. The VQ was used to identify the typical F/T associated with each one of the tool/tissue interactions in the surgery "*dictionary*," or using the language analogy, it characterized different pronunciations of a word. Utilizing the "*dictionary*" of surgery, the MM was then used to define the process of each step of the surgical procedure, or in other words, "*dictating chapters*" of the surgical "*story*."

1) Video Analysis: The VA was performed by two expert surgeons encoding the video of each step of the surgical procedure frame by frame (NTSC—30 frames/s). The encoding process used a code-book of 14 different discrete tool maneuvers in which the endoscopic tool was interacting with the tissue (Table II). Each identified surgical tool/tissue interaction, had a unique F/T pattern. For example, in the laparoscopic cholecystectomy, isolation of the cystic duct and artery involves performing repeated pushing and spreading maneuvers (PS-SP—Table II), which are accomplished by applying pushing forces mainly along the Z axis (F_z) and spreading forces (F_g) on the handle.

The 14 tool/tissue interactions can be further divided into three types based on the number of movements performed simultaneously. The fundamental maneuvers are defined as Type I. The "idle" state was defined as moving the tool in space (abdominal cavity) without touching any internal organ. The

(a)

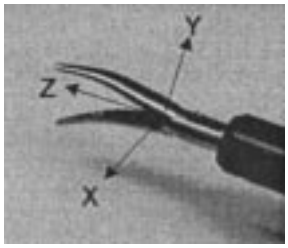

(b)

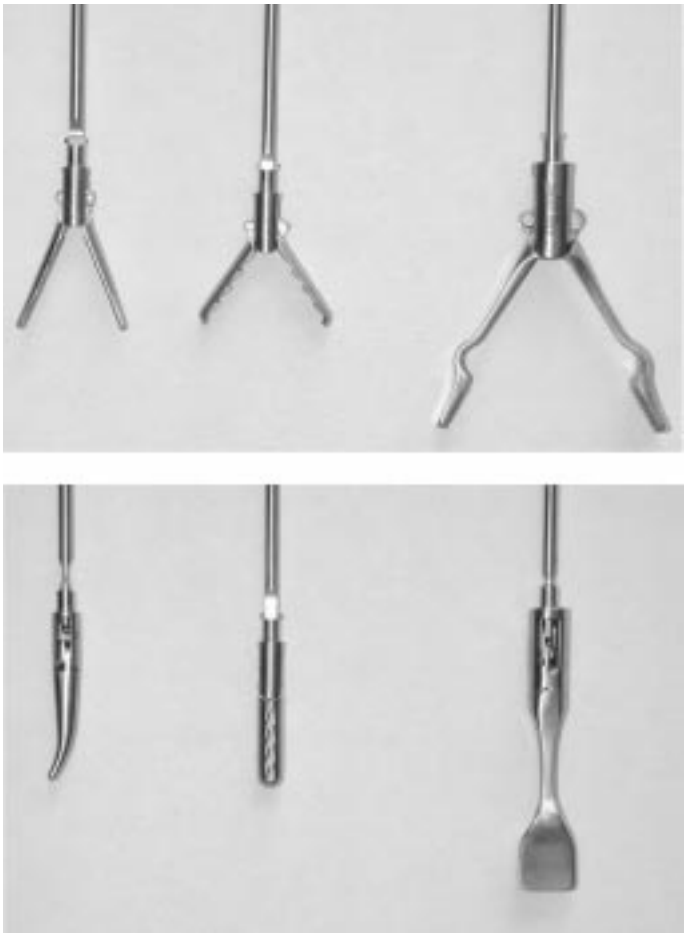

(c)

Fig. 3. The instrumented endoscopic grasper: (a) The grasper with the three axis F/T sensor implemented on the outer tube and a force sensor located on the instrument handle. (b) The tool tip and X, Y, Z frame aligned with the three axis F/T sensor. (c) Tool tips used in the surgical procedure (from left to right): Atraumatic Grasper, Babcock grasper, Curved dissector.

forces and torques developed in this state represent mainly the interaction with the trocar and the abdominal wall, in addition to the gravitational and inertial forces. In the "grasping" and "spreading" states, compression and tension were applied to the

TABLE I
DEFINITIONS OF SURGICAL PROCEDURE STEPS AND TYPES OF THE TOOL TIPS THAT WERE USED (SHADED STEPS PERFORMED BUT NO FORCE/TORQUE DATA WERE RECORDED)

Procedure	Step	Description	Tool Type	Hand	Video F/T
Laparoscopic Cholecystectomy	LC - 1	Positioning Gall Bladder	Atraumatic Grasper	L	+
	LC - 2	Exposure of Cyctic Duct	Curved Dissector	R	+
	LC - 2*	Divide of Cyctic Duct	Scissors	R	-
	LC - 3	Dissection of Gall Bladder Fossae	Curved Dissector	R	+
	LC - 4	Exposure of Cystic Artery	Curved Dissector	R	-
	LC - 4*	Dividing Artery	Scissors	R	-
Laparoscopic Nissen Fundoplication	LNF - 1	Dissect Right Crus	Surgiwand	R	-
	LNF - 2	Dissect Left Crus	Surgiwand	R	-
	LNF - 3	Dissect Esophagus / Blunt	Curved Dissector	R	+
	LNF - 4	Placing a Wrap Around the Esophagus	Babcock Grasper	R	+
	LNF - 5	Suture Wrap / Intracorporeal Knot Tying With Needle Holder	Curved Dissector	R	+
	LNF - 6	Coronal Sutures / Intracorporeal Knot Tying Endostitch	Endostitch	R	-

TABLE II
DEFINITION OF TOOL/TISSUE INTERACTIONS AND THE CORRESPONDING DIRECTIONS OF FORCES AND TORQUES APPLIED DURING MIS

Type	State Name	State Acronym	Force / Torque						
			Fx	Fy	Fz	Tx	Ty	Tz	Fg
I	Idle	ID	*	*	*	*	*	*	*
	Grasping	GR							+
	Spreading	SP							-
	Pushing	PS			-				
	Sweeping (Lateral Retraction)	SW	+/-	+/-		+/-	+/-		
II	Grasping - Pulling	GR-PL			+				+
	Grasping - Pushing	GR-PS			-				+
	Grasping - Sweeping (Grasping - Lateral Retraction)	GR-SW	+/-	+/-		+/-	+/-		+
	Pushing - Spreading	PS-SP			-				-
	Pushing - Sweeping	PS-SW	+/-	+/-	-	+/-	+/-		
	Sweeping - Spreading	SW-SP	+/-	+/-		+/-	+/-		-
III	Grasping - Pulling - Sweeping	GR-PL-SW	+/-	+/-	+	+/-	+/-		+
	Grasping - Pushing - Sweeping	GR-PS-SW	+/-	+/-	-	+/-	+/-		+
	Pushing - Sweeping - Spreading	PS-SW-SP	+/-	+/-	-	+/-	+/-		-

tissue by closing and opening the grasper handle, respectively. In the "pushing" state, the tissue was compressed by moving the tool along the Z axis. "Sweeping" consisted of placing the tool in one position while rotating it around the X and/or Y axes (trocar frame). The rest of the tool/tissue interactions in Types II and III were combinations of the fundamental ones in Type I.

2) Vector Quantization: The second type of analysis used the K-mean VQ algorithm to encode the continuous multi-

dimensional F/T data (F_x, F_y, F_z, T_x, T_y, T_z, and F_g) into discrete symbols representing F/T cluster centers (signatures). This step of the data analysis was essential for using the discrete version of MM. During the first step of VQ analysis the seven-dimensional F/T data vector was reduced to a five–dimensional (5-D) vector by calculating the magnitude of the force and torque in the XY plane (F_{xy}, T_{xy}). Although it may appear that information about the direction of the F/T in the XY plane was lost during this data reduction, this process actually canceled out differences between surgeons due to variations in standing position relative to the animal.

Given M patterns $\overline{X}_1, \overline{X}_2, \ldots, \overline{X}_M$ contained in the pattern space $\overline{S}$, the process of clustering can be formally stated as seeking the regions $\overline{S}_1, \overline{S}_2, \ldots, \overline{S}_K$ such that every data vector $\overline{X}_i$ ($i = 1, 2, \ldots, M$) falls into one of these regions and no $\overline{X}_i$ is associated in two regions, i.e.,

$$\overline{S}_1 \cup \overline{S}_2 \cup \overline{S}_3 \cdots \cup \overline{S}_K = \overline{S} \tag{1a}$$

$$\overline{S}_i \cap \overline{S}_j = 0 \qquad \forall i \neq j. \tag{1b}$$

The K-means algorithm, is based on minimization of the sum of squared distances from all points in a cluster domain to the cluster center,

$$\min \sum_{X \in S_j(k)} (\overline{X} - \overline{Z}_j)^2 \tag{2}$$

where $S_j(k)$ was the cluster domain for cluster centers $\overline{Z}_j$ at the kth iteration, and $\overline{X}$ was a point in the cluster domain.

The pattern spaces $\overline{S}$ in the current study were composed from the F/T applied on the surgical tool by the surgeon for different tool/tissue interactions. A typical data vector $\overline{X}_i$ was a 5-D vector defined as $\{F_{xy}, F_z, T_{xy}, T_z, F_g\}$. The cluster regions $\overline{S}_i$ represented by the cluster centers $\overline{Z}_j$, defined typical F/T signatures associated with a specific tool/tissue interaction (e.g., PS, PL, GR, etc.). The number of clusters identified in each type of tool/tissue interaction was based on the squared-error distortion criterion [see (3)]. As the number of clusters increased the distortion decreased exponentially. Following this behavior, the number of clusters was constantly increased until the squared-error distortion gradient as a function of k decreased below a threshold of 1%

$$d(\overline{X}, \overline{Z}) = ||\overline{X} - \overline{Z}_j||^2 = \sum_{i=1}^{k} (\overline{X} - \overline{Z}_i)^2. \tag{3}$$

The cluster centers $\overline{Z}_j$ for each tool/tissue interaction (Table II) forming a code-book were then used to encode the entire database of the actual surgical procedures converting the continuous multidimensional data into a one-dimensional (1-D) vector of finite symbols representing F/T signatures.

3) Markov Model (MM): The third and final step of the data analysis was to develop the MM and the methodology for evaluating surgical skill in MIS. The MM was found to be a very compact method to statistically summarize a relatively complex task such as a step of a MIS procedure. Moreover, the skill level was implemented into the MM by developing different MMs based on data acquired for expert surgeons and NS performing the different steps of the MIS procedures.

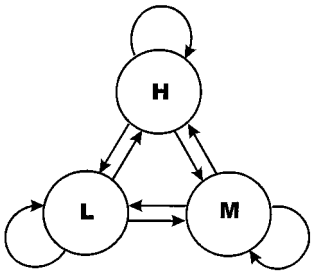

Fig. 4. Fully connected three-state MM architecture. The observation symbols of each state were selected based on the F/T magnitudes (H—High, M—Medium, L—Low).

a) Hidden Markov Model Definitions (HMM): From the mathematical perspective, the model developed in the current study was a MM. However, some of the mathematical notations, used for developing the surgical skill scale, were inspired by the HMM theory. For that reason a short review based on [29] was given for providing the basic terminology and defining the problems associated with the HMM.

Five elements should be defined in order to specify a HMM $\lambda = (A, B, \pi)$ [29]: 1) the number of states in the model—N; 2) the number of distinct observation symbols per state—M; 3) the state transition probability distribution—A; 4) the observation symbol probability distribution—B; and 5) the initial state distribution—π.

Given the HMM architecture, there are three basic problems of interest [29]: 1) the evaluation problem; 2) uncover the hidden states problem; and 3) the training problem. Out of the three problems only the evaluation, problem i), was applicable to the MM model developed in the current study. This is due to the fact that the MM states were not hidden and could be identified by the VQ analysis. The evaluation problem 1) involves computing the probability $P(O|\lambda)$ of the observation sequence $O = o_1, o_2, \ldots, o_T$ given the model $\lambda = (A, B, \pi)$ and the observation sequence.

b) Markov Model (MM) Architecture: For reasons that would be further discussed in Section III-C, the selected MM had a fully connected three-state architecture. The VQ cluster centers, representing the F/T signatures of each one of the 14 tool/tissue interaction (Table II), were divided into three groups according to their F/T magnitudes (H—high, M—medium, L—low). All the F/T signatures out of the 14 tool/tissue interactions associated with the H, M, and L groups were then lumped to form the three states of the MM.

One of the fundamental requirements regarding the MM architecture was that MMs representing surgeons with different skill level should share the same model architecture (Fig. 4). This feature allowed quantitative comparison of MMs representing different skill level in terms of statistical similarities. Moreover, the three-state architecture was based on the assumption that F/T magnitudes were one of the major differences between surgical skill levels, an assumption that was further supported by the experimental results (Section III-C).

Each state in the MM had a unique set of observation symbols (F/T signatures). Under this condition, each F/T signature corresponded only to a specific state of the MM and, therefore, the VQ encoding analysis alone was sufficient for

identifying the MMs' states. Therefore the matrices A, B, π (problem ii) and the states sequence (problem iii) could be computed in a straightforward manner rather then using the training algorithms. However, the evaluation problem (problem i) still had to be solved by using the Forward–Backward procedure incorporating the scaling process [29].

As described in Section II-C, ten subjects (two groups: NS, and ES) performed two MIS procedures which were further divided into steps. Using the given MM architecture and the encoded F/T signals, two MMs were trained for each step of the surgical procedures, representing the performances of three subjects out of five in each group (NS and ES), and further referred to as the NS-MM (λ_{NS}) and the ES-MM (λ_{ES}), respectively. The MMs developed based on the data of the two remaining subjects in each group (λ_i) and their encoded F/T signals (observation vectors—O_i) were used to define the skill scale based on the statistical similarity to the main groups (λ_{NS}, λ_{ES}). This procedure is schematically described in Fig. 5.

Two statistical similarity factors were defined as follows:

$$NSF = \log(\mathbf{P}(O_i|\lambda_{\mathrm{NS}}))/\log(\mathbf{P}(O_i|\lambda_i))$$
$$ESF = \log(\mathbf{P}(O_i|\lambda_{\mathrm{ES}}))/\log(\mathbf{P}(O_i|\lambda_i)). \quad (4)$$

The NSF defined the statistical similarity between the performances of the subject under study and the NS group, whereas the ESF indicated the statistical similarity relative to the ES group. These two factors provided the major classification parameters for evaluating surgical skill in MIS. The NSF and ESF form a two-dimensional (2-D) subspace with values in the range of $\langle 0, 1\rangle$. In this subspace, an absolute NS would be represented by $NSF = 1$ and $ESF = 0$, and vice versa for an absolute ES. In this 2-D subspace, the line $NSF = ESF$ represented the boundary between the expert region ($ESF > NSF$) and the novice region ($ESF < NSF$). The line $NSF = ESF$ was only one line out of a group of lines representing iso-performances. It is possible to define an iso-performance line such that all the points (ESF_i, NSF_i) on the line have a constant ratio (C) between the squared distance to the points (0, 1) (absolute NS) and the squared distance to the point (1, 0) (absolute ES) (5). This transforms the 2-D subspace into a 1-D scale

$$C = \{d((ESF_i, NSF_i), (0, 1))/d((ESF_i, NSF_i), (1, 0))\}^2 \quad (5a)$$

$$C = \frac{(1 - ESF_i)^2 + NSF_i^2}{ESF_i^2 + (1 - NSF_i)^2}. \quad (5b)$$

III. Results

A. Tool/Tissue Interaction States and Transition—Expert Analysis

Analyzing videotapes of the surgical procedures incorporated the visual view of the tool/tissue interaction and graphs of the F/T at the tool/hand interface frame by frame allowed to define the primary tool/tissue interactions in the two MIS procedures and the direction of forces and torques associated with them [Table II, Fig. 3(b)]. Once these tool/tissue interaction archetypes were defined, each step of the surgical procedure could be manually analyzed into a list of tool/tissue interaction.

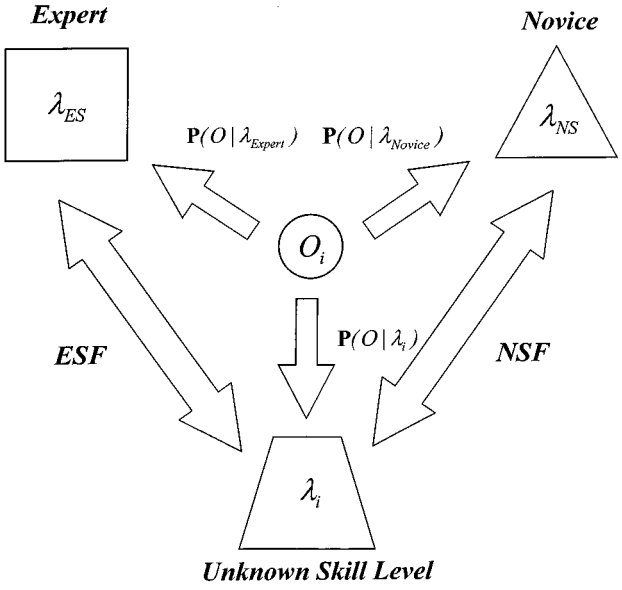

Fig. 5. Skill evaluation using Markov model classification—Comparing statistical similarities between the performance of a surgeon with an undefined skill level to the experts and novices surgeon groups.

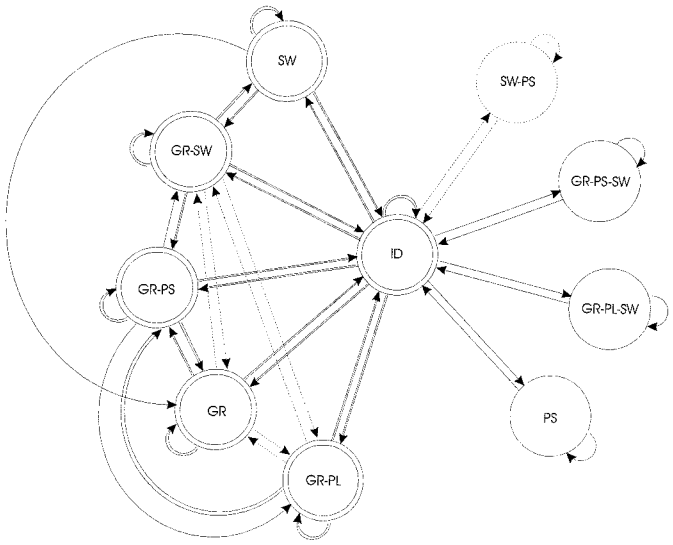

Fig. 6. State transitions diagram of placing wrap around the esophagus during laparoscopic Nissen fundoplication (solid line: ES; dashed line: NS; doubled line: both).

This list was further transformed into a more compact diagram (as shown in Fig. 6) defining a typical tool/tissue transition diagram of a surgical procedure in MIS. The tool/tissue transition diagram depicted in Fig. 6 represented the surgical step in which a wrap was placed around the esophagus during a laparoscopic Nissen fundoplication (Table I, LNF-4). Although Fig. 6 illustrates a unique/tool tissue transition diagram of a MIS procedure step, the star-shaped architecture was similar to all the other MIS steps under study.

The center state of the star shaped tool/tissue transition diagram (Fig. 6) included the idle state. This state, in which no tool/tissue interaction was performed, was mainly used by both ES and NS to move from one operative state to the other. However, the expert surgeons used the idle state only as a transition

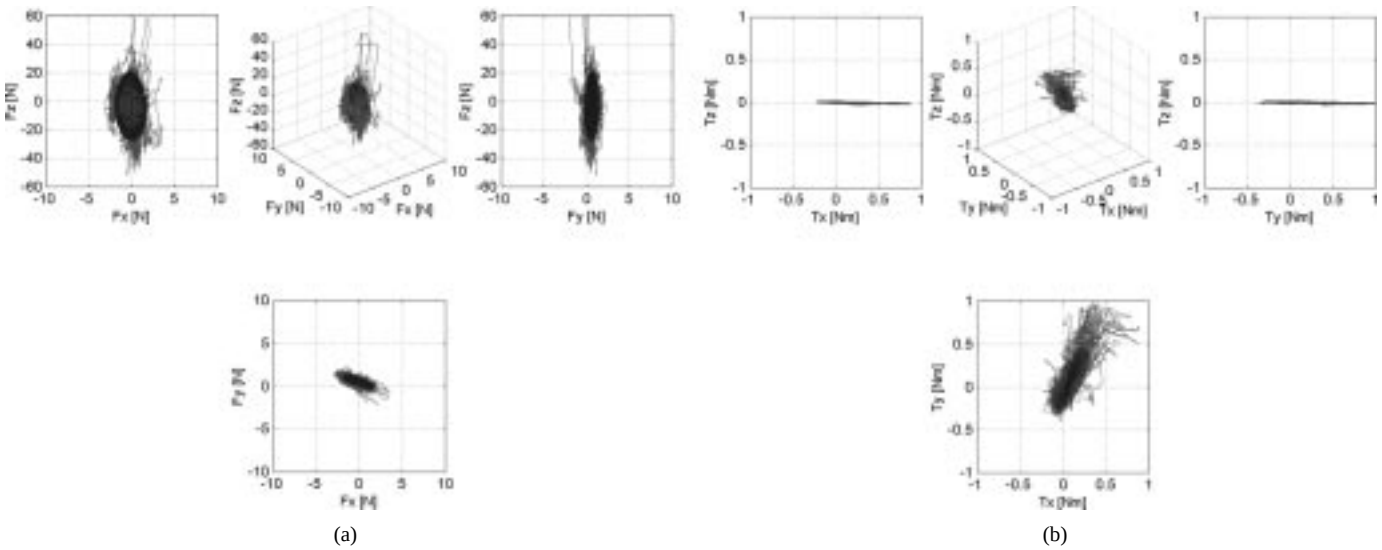

(a) (b)

Fig. 7. Forces and torques measured at the human/tool interface while dissecting the gallbladder fossae during laparoscopic cholecystectomy. For the definitions of the X, Y, and Z directions, see Fig. 3(b). (a) Forces and (b) torques.

state while the novices spent significant amount of time in this state planning the next tool/tissue interaction. Another major difference between ES and NS was related to the tool/tissue interaction and tool/tissue transitions used by these two groups. Essentially Fig. 6 was composed from two separate models representing the ES model (double line and solid line) and the NS (double line and dashed line). For the purpose of evaluating surgical skills, the model representing the NS and the one representing the ES must share the same architecture. This requirement led to redefining the model states and architecture as described previously in Section II-C3.

B. Force/Torque Signatures

Typical raw data of forces and torques were plotted in a 3-D space showing the loads developed at the sensor location while dissecting the gallbladder fossae for 425 sec by an expert surgeon during laparoscopic cholecystectomy (Fig. 7). The black ellipsoid is a region that includes 95% of the F/T samples. The forces along the Z axis (in/out of the trocar) were higher compared with the forces in the XY plane. On the other hand, torques developed by rotating the tool around the Z axis were extremely low compared with the torques generated while rotating the tool along the X and Y axis while sweeping the tissue or performing lateral retraction. Similar trends in terms of the F/T magnitude ratios between the X, Y, and Z axes were found in the data measured in other steps of the MIS procedures.

Fig. 7 provided a general overview of the F/T magnitudes applied during MIS, however, gaining a deeper insight into the processes of MIS was obtained by using the VQ analysis. Following the protocol described in Section II-C2, 87 different F/T signatures (cluster centers) were identified for the different tool/tissue interactions. For example, Fig. 8 represented nine F/T signatures (VQ code words) associated with the pushing-sweeping-spreading (Table II—PS-SW-SP) tool/tissue interaction. These nine signatures were dominated by negative values of F_z (pushing), T_{xy} (sweeping the tissue in the XY plane) and negative values of F_g (spreading). These nine pentagonal cluster centers found in the PS-SW-SP F/T data

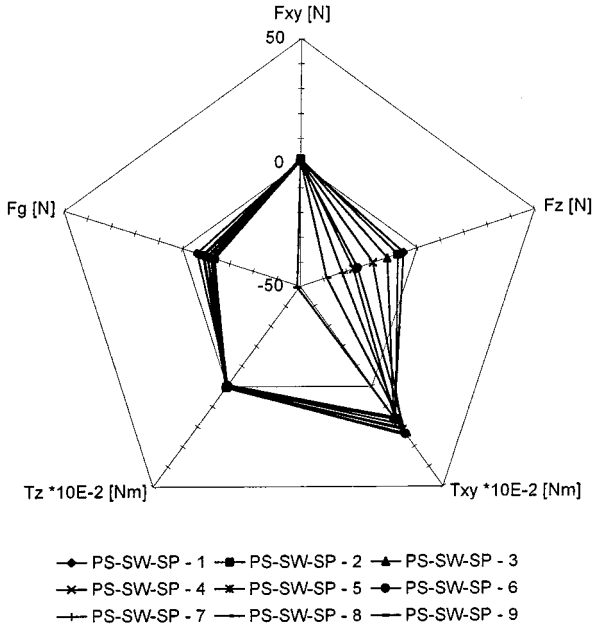

Fig. 8. A typical F/T signatures (cluster centers) measured at the human/tool interface and associated pushing-sweeping-spreading tool/tissue interaction in MIS.

may represent the entire F/T at this specific tool/tissue interaction. The rest of the data associated with PS-SW-SP might be considered as a variation of these nine themes and can be correlated to one of these signatures using the criterion defined by (3). Moreover, further analysis of entire code-book (87 F/T signatures) showed no overlap between signatures. There was at least one dimension (out of the five) that differentiated each signature from the others.

Once the code-book was defined, the entire database was encoded into the 87 F/T signatures. This encoding process allowed exploration of a new aspect regarding the differences between NS and ES. This new aspect was related to the magnitudes of F/T applied by NS and ES during each step of the MIS procedures for the different tool/tissue interactions (Table II).

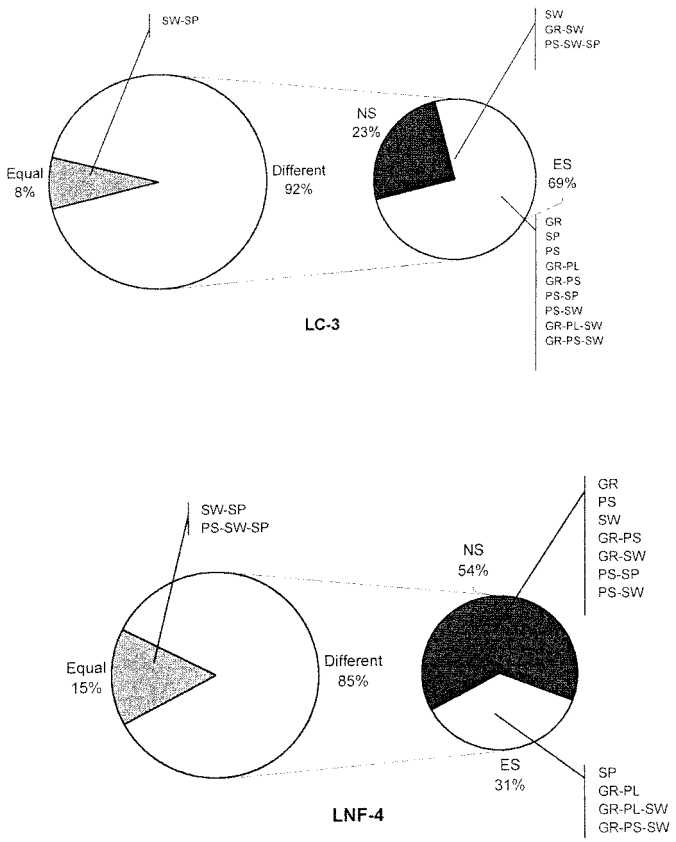

Fig. 9. F/T magnitude distributions at different tool/tissue interactions applied by NS and ES during steps of an endoscopic surgical procedures (For details see Table I). The pie bar on the left-hand side shows the distribution of tool/tissue interactions in which significant differences ($p < 0.05$)—dotted sector, and nonsignificant differences ($p > 0.05$) gray sector in terms of the F/T magnitudes were applied by NS and ES. In tool/tissue, interactions were significant differences were identified between NS and ES (Dotted sector), the pie diagram on the right-hand side shows the correspondence between high F/T magnitudes and the group of surgeons who applied them (black sector: NS; and white sector: ES).

The entire F/T database was lumped into two groups e.g., the NS group and ES group. The distribution of the F/T signature for each tool/tissue interactions were then calculated for the NS and ES groups performing the different steps of the MIS procedures. The distributions of the F/T signatures applied by the NS and the ES were tested using the median test (nonparametric method) combined with the fourfold point statistical procedure [30] to identified tool/tissue interactions in which the F/T magnitude distributions of the two groups were significantly different. This analysis showed that the F/T magnitudes applied by the NS and ES in most of the tool/tissue interactions were significantly different ($p < 0.05$) (Fig. 9).

Each one of the F/T magnitude distribution for two different surgical steps were represented in Fig. 9 by two pie diagrams. The pie diagram on the left-hand side defined the tool/tissue interactions in which no significant difference was found (gray sector) between NS and ES and cases where significant difference was observed (dotted sector). When a significant difference was identified, the pie diagram on the right-hand side showed which group (NS—black sector, or ES—white sector) applied higher magnitudes of F/T in each one of the tool/tissue interactions. For example, in laparoscopic cholecystectomy Step 3 (Fig. 9—LC-3) no significant difference in the F/T magnitude

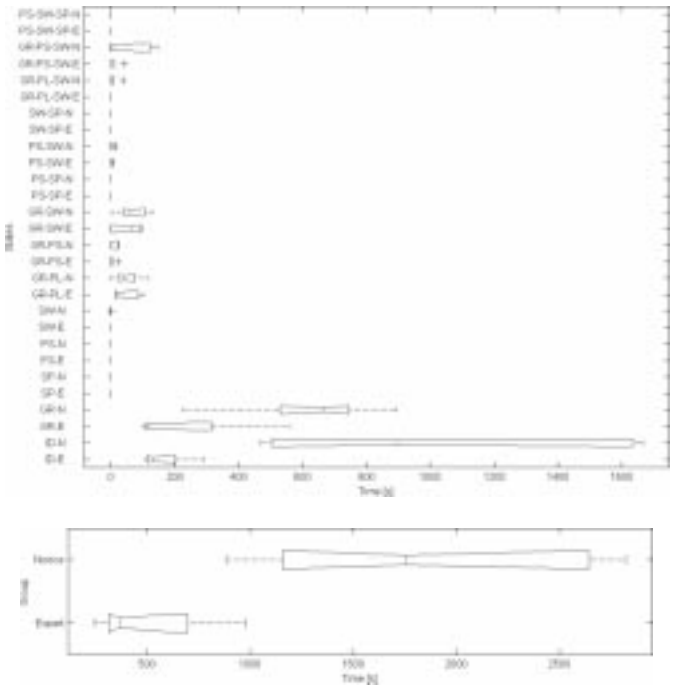

Fig. 10. Time spent at each tool/tissue interaction by NS and ES while performing suture wrap and intracorporeal knot tying with needle holder. The time distribution in each tool/tissue interaction of the ten subjects is represented by a notch box plot. The lower and upper lines of the box are the 25th and 75th percentiles of the sample representing the interquartile range. The line in the middle of the box is the sample median. The notches in the box depicts the 95% confidence interval about the median of the sample. The lines extending above and below the box define the 95 percentiles of the sampled data.

was identified in SW-SP which was 8% of all the tool/tissue interactions. In all the other 92% of tool/tissue interactions, significant difference was identified (left-hand pie chart). Out of the cases where significant difference was observed, in 23% of the tool/tissue interactions (e.g., SW, GR-SW, and PS-SW-SP) the NS applied higher F/T magnitudes compare with the ES and in 69% of the cases (e.g., GR, SP, PS, GR-PL, etc.) the ES applied higher F/T magnitudes compare with the NS (right-hand pie chart).

In general, a significant difference was identified in most of the tool/tissue interactions. Moreover, when the six surgical steps were divided according to the nature of the tool/tissue interactions—e.g., 1) tissue dissection (LC-2, LC-3, and LNF-3); 2) tissue manipulation (LC-1, LNF-4)—the results showed that higher magnitudes of F/T were applied by the ES compared with the NS when dissecting the tissues, whereas lower magnitudes of F/T were applied by the ES compared with the NS when manipulating the tissues.

Completion time of each surgical step was another criterion of surgical skill. Studying the median completion time of the NS group and ES group showed a significant difference between these groups ($p < 0.05$). The surgical procedure's completion time was longer for the NS by a factor of 1.5–4.8 compared with the ES. The difference between NS and ES was more profound in steps requiring higher dexterity and manual skill (e.g., LNF-5) compared with steps where a specific organ was placed in a specific position (e.g., LC-1). Moreover, the VA and VQ encoding allowed evaluation of the time intervals spent performing different tool/tissue interaction (Fig. 10). The main factor con-

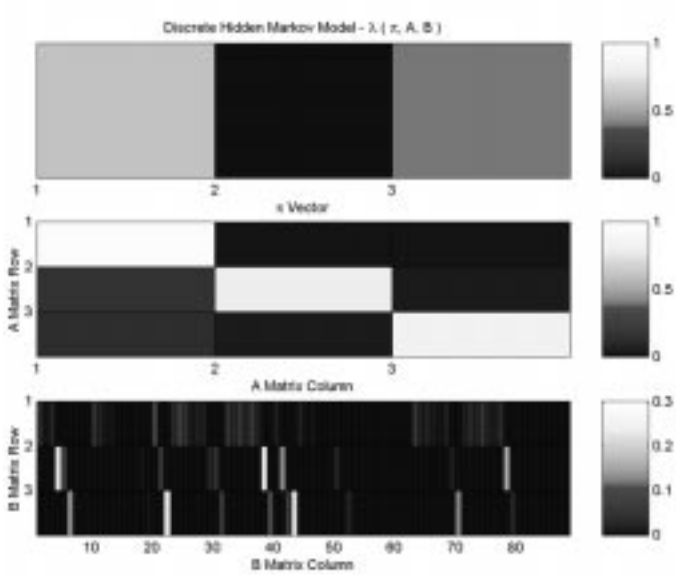

Fig. 11. Graphical representation of a three-state fully connected MM defining the step of positioning gallbladder during Laparoscopic Cholecystectomy performed by NS.

tributing to the significant difference in the completion times between NS and ES was the time spent in the "idle" state. The NS spent significantly more time in the idle state compare with the ES.

C. MM and the MIS Skill Scale

A typical MM representing the step of positioning the gallbladder (LC-1) performed by NS was depicted in Fig. 11. This plot rendered the probability of each element of the matrices A, B, π as a color values, defining the three states of a fully-connected MM. Similar MMs were developed for the NS group, the ES group, and the four remaining subjects (two NS and two ES) for each step of the surgical procedures. According to the π vector, defining the initial state distribution, it was more likely the surgeon would start with state 1 (L—Low in Fig. 4), which was associated with the highest probability (π_1). Once the surgeon was in a certain state (L, M, or H) it was more likely that he or she would stay in the same state rather then move to another state. This phenomenon was demonstrated by the high probability values along the diagonal (a_{ii}) compared with the nondiagonal probability values (a_{ij}) of the state transition probability matrix A. Moreover, transitions from the M state to the L state ($M \Rightarrow L$)—$a_{21}$and from the H state to the L ($H \Rightarrow L$)—a_{31} were more frequent than the reverse state transitions—a_{23} and a_{32}. Thus, once the surgeon was in state L, the probability of moving to state M (a_{12}) was almost equal to the probability of moving to state H (a_{13}). Using a unique subset of symbols from the 87 symbols code-book for each MM state was exhibited by the fact that there was no overlap between the rows of the B matrix.

The skill analysis performed by using MMs of two NS and two ES performing LC and LNF was summarized as a scatter plot in Fig. 12(a) representing the NSF and the ESF probability [see (5)]. The solid line ($NSF = ESF$) represented the boundary between the NS (top-left) and the ES (bottom-right). Except for three cases, where ES were misclassify as NS, the MMs were capable of classifying NS and ES correctly in terms of statistical similarity into their respective groups.

Dotted lines in Fig. 12(a) indicate iso-performances (in addition to the solid line indicating the boundary between NS and ES). Each iso-performance line was defined by a different C value [see (5)], and therefore all the points along this line had the same squared distance ratio between the points: (0, 1) and (1, 0) [see (5)]. Using the iso-performance parameter C, the 2-D performance domain [Fig. 12(a)] was mapped into a 1-D performance scale [Fig. 12(b)] such that each iso-performance line defined by the C parameter was converted into a point along the 1-D performance scale. On the C scale the ES region and NS region were defined as $\langle 0, 1\rangle$ and $\langle 1, \infty\rangle$ correspondingly, whereas the value one represents the boundary between ES and NS. Although the range of the C scale by definition was from 0 to infinity, practically all the data points lay between 0.65 and 1.6. As demonstrated in Fig. 12(b), the C skill scale differentiates the performance of the NS from the ES for the MIS procedure under study.

IV. Conclusion

Minimally invasive surgery is a complex task that requires a synthesis between visual and haptic information. Analyzing MIS in terms of these two sources of information is a key step toward developing objective criteria for training surgeons and evaluating the performance of a master/slave robotic or teleoperated system and VR simulations with haptic devices. Synthesizing the visual and haptic information indicates five areas in which the novice surgeon (NS) group was different from the expert surgeon (ES) group when performing MIS: 1) types of tool/tissue interaction being used, 2) transitions between tool/tissue interactions being applied, 3) time spent while performing each tool/tissue interaction (especially the idle state), 4) overall completion time, and 5) F/T magnitudes being applied by the surgeons on the endoscopic tools.

All the criteria differentiating skill level between NS and ES described above were found to be related. In general, it took the expert surgeon less time to perform a typical MIS compared with the novice surgeon, who spent most of the extra time in the "idle" state. This probably results from a number of factors including advanced knowledge of the anatomy, higher level of hand-eye coordination, and/or greater experience in handling the endoscopic surgical instrument. The magnitude of F/T applied by NS and ES varied based on the task being performed. Higher F/T magnitudes were applied by NS compared with ES when performing tissue manipulation. This might be a result of insufficient dexterity of the NS that might represent a potential for tissue damage and time consumption. However, low F/T magnitudes were applied by the NS compared with the ES during tissue dissection, which might indicate excessive caution to avoid irreversible tissue damage. More dissection movements were required to be performed by the NS in order to tear the tissue, a process which substantially decreases the efficiency of the MIS procedure and increases the completion time. Moreover, using the F/T information in real-time during the course of learning as feedback information to the NS may improve the

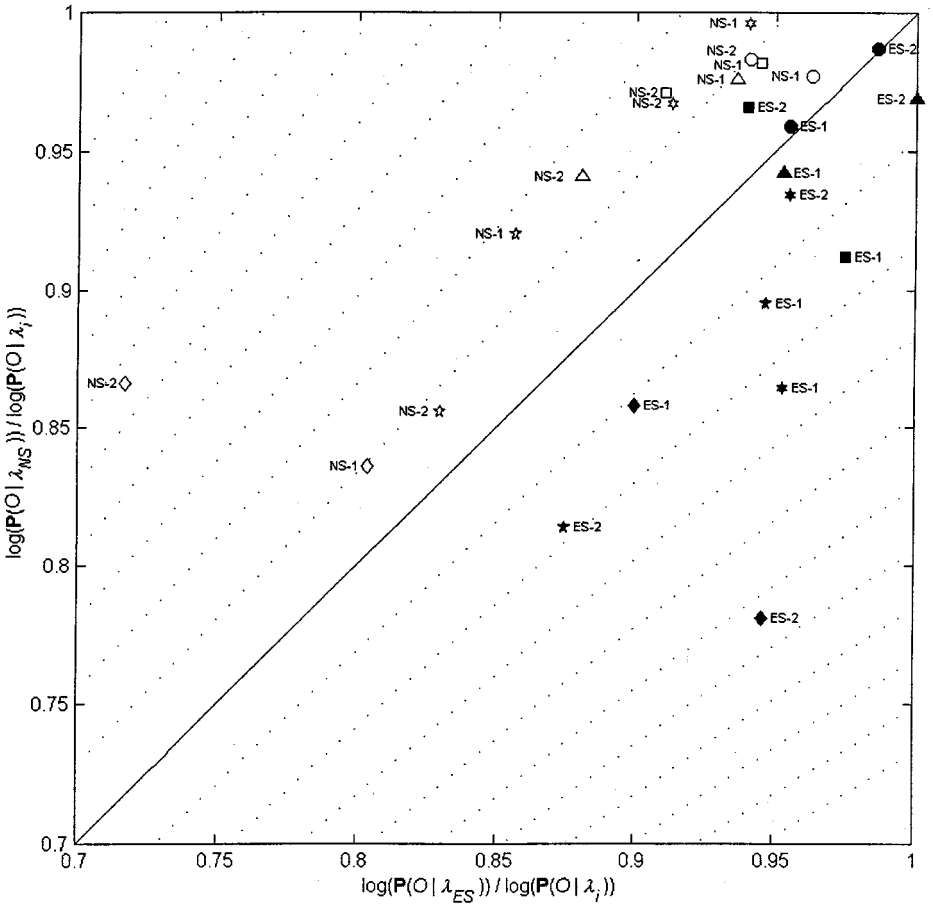

(a)

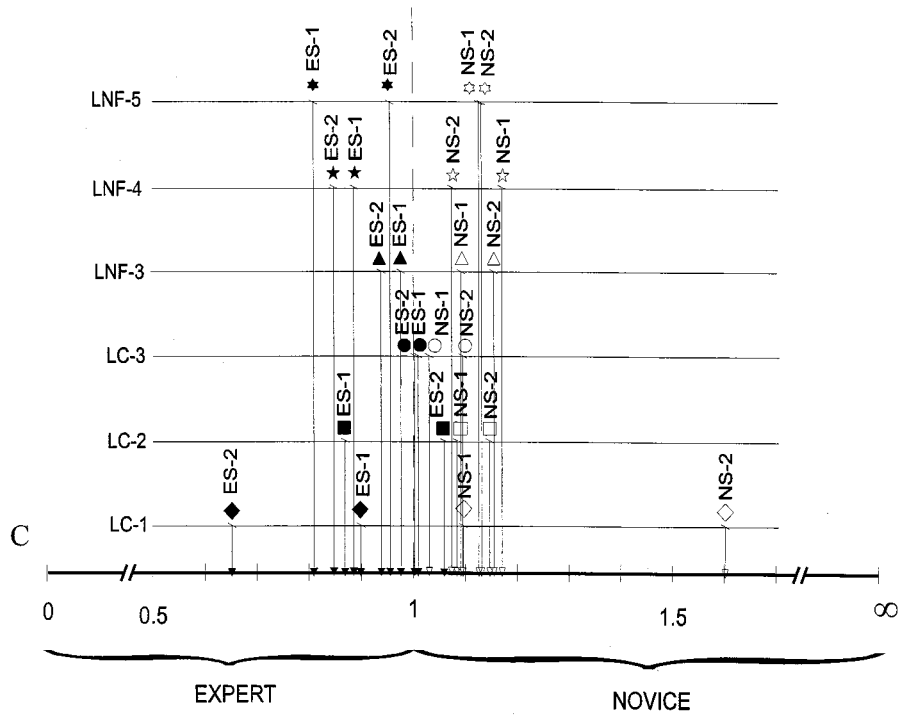

(b)

Fig. 12. Performance scales of two expert surgeons (ES-1 and ES-3: hollow icons) and two novice surgeons (NS-1 and NS-2: filled icons) performing laparoscopic Cholecystectomy (♦: LC-1; ■: LC-2; and •: LC-3) and laparoscopic Nissen Fundoplication (▲: LNF-3; ★: LNF-4; and ✸: LNF-5). (a) Scatter plot of the performance parameters NSF as a function of ESF [see (4)]. (b) One-dimensional performance scale representing the C parameter [see (5)].

learning process, reduce soft tissue injury, and increase the efficiency during endoscopic surgery.

The multidimensional information acquired during MIS was integrated into a single model using the MM approach. The MM was found to be a very compact yet comprehensive and powerful tool to model the complexity of MIS. Incorporating MM in the surgical skill analysis allowed objective quantification of skill defined as the statistical similarity of a data measured from a subject with apparently unknown skill level to the NS and ES models. Using these techniques, 87.5% of the surgical procedures were correctly classified into the NS and ES groups. The 12.5% of the procedures that were misclassified were performed by the ES and classified as NS. However, in these cases the performance index values were very close to the NS/ES boundary.

The approach outlined in this study could be extended by increasing the size of the database to include more surgical procedures performed by more surgeons. Our ongoing research in this field is focused on evaluating and tracking skill level of surgeons during their residency using the proposed method. This information, combined with other feedback data (e.g., tool position), may be used as a basis to develop teaching techniques for optimizing tool usage in MIS. A well-established methodology for evaluating skill level would allow NS to practice outside of the operating room on animal models or using realistic VR simulators until they had achieved a desired level of competence and compare themselves to norms established by experienced surgeons and licensing organizations.

REFERENCES

[1] A. M. Derossis, G. M. Fried, M. Abrahamowicz, H. H. Sigman, J. S. Barkun, and J. L. Meakins, "Development of a model for training and evaluation of laparoscopic skills," *Amer. J. Surg.*, vol. 175, no. 6, pp. 482–487, Jun. 1998.

[2] J. C. Rosser Jr., L. E. Rosser, and R. S. Savalgi, "Objective evaluation of a laparoscopic surgical skill program for residents and senior surgeons," *Arch. Surg.*, vol. 133, no. 6, pp. 657–661, Jun. 1998.

[3] B. M. Wolfe, Z. Szabo, M. E. Moran, P. Chan, and J. G. Hunter, "Training for minimally invasive surgery. Need for surgical skills," *Surg. Endosc.*, vol. 7, no. 2, pp. 93–95, Mar.–Apr. 1993.

[4] D. Ota, B. Loftin, T. Saito, R. Lea, and J. Keller, "Virtual reality in surgical education," *Comput. Biol. Med.*, vol. 25, no. 2, pp. 127–137, Mar. 1995.

[5] N. Taffinder, C. Sutton, R. J. Fishwick, I. C. McManus, and A. Darzi, "Validation of virtual reality to teach and assess psychomotor skills in laparoscopic surgery: Results from randomised controlled studies using the MIST VR laparoscopic simulator," *Stud. Health Technol. Inform.*, vol. 50, pp. 124–130, 1998.

[6] A. G. Gallagher, N. McClure, J. McGuigan, I. Crothers, and J. Browning, "Virtual reality training in laparoscopic surgery: A preliminary assessment of minimally invasive surgical trainer virtual reality (MIST VR)," *Endoscopy*, vol. 31, no. 4, pp. 310–313, May 1999.

[7] R. V. O'Toole, R. R. Playter, T. M. Krummel, W. C. Blank, N. H. Cornelius, W. R. Roberts, W. J. Bell, and M. Raibert, "Measuring and developing suturing technique with a virtual reality surgical simulator," *J. Amer. Coll. Surg.*, vol. 189, no. 1, pp. 114–127, Jul. 1999.

[8] T. Mori, N. Hatano, S. Maruyama, and Y. Atomi, "Significance of 'hands-on training' in laparoscopic surgery," *Surg. Endosc.*, vol. 12, no. 3, pp. 256–260, Mar. 1998.

[9] M. MacFarlane, J. Rosen, B. Hannaford, C. Pellegrini, and M. Sinanan, "Force-feedback grasper helps restore sense of touch in minimally invasive surgery," *J. Gastrointest. Surg.*, vol. 3, no. 3, pp. 278–285, May 1999.

[10] J. Rosen, B. Hannaford, M. MacFarlane, and M. Sinanan, "Force controlled and teleoperated endoscopic grasper for minimally invasive surgery—Experimental performance evaluation," *IEEE Trans. Biomed. Eng.*, vol. 46, pp. 1212–1221, Oct. 1999.

[11] M. Downes, M. C. Cavusoglu, W. Gantert, L. W. Way, and T. Tendick, "Virtual environments for training critical skills in laparoscopic surgery," *Stud. Health Technol. Inform.*, vol. 50, pp. 316–322, 1998.

[12] C. S. Tseng, Y. Y. Lee, Y. P. Chan, S. S. Wu, and A. W. Chiu, "A PC-based surgical simulator for laparoscopic surgery," *Stud. Health Technol. Inform.*, vol. 50, pp. 155–60, 1998.

[13] J. Berkely, S. Weghorst, H. Gladstone, G. Raugi, and M. Ganter, "Fast finite element modeling for surgical simulation," *Stud. Health Technol. Inform.*, vol. 62, pp. 55–61, 1999.

[14] R. Satava, "Virtual reality surgical simulator," *Surg. Endosc.*, vol. 7, pp. 203–205, 1993.

[15] D. Ota, B. Loftin, T. Saito, R. Lea, and J. Keller, "Virtual reality in surgical education," *Comput. Biol. Med.*, vol. 25, pp. 127–137, 1995.

[16] M. Noar, "Endoscopy simulation: A brave new world?," *Endoscopy*, vol. 23, pp. 147–149, 1991.

[17] C. S. Tseng, Y. Y. Lee, Y. P. Chan, S. S. Wu, and A. W. Chiu, "A PC-based surgical simulator for laparoscopic surgery," *Stud. Health Technol. Inform.*, vol. 50, pp. 155–160, 1998.

[18] H. Delingette, S. Cotin, and N. Ayache, "Efficient linear elastic models of soft tissues for real-time surgery simulation," *Stud. Health Technol. Inform.*, vol. 62, pp. 100–101, 1999.

[19] C. Basdogan, C. H. Ho, and M. A. Srinivasan, "Simulation of tissue cutting and bleeding for laparoscopic surgery using auxiliary surfaces," *Stud. Health Technol. Inform.*, vol. 62, pp. 38–44, 1999.

[20] E. Heer and A. K. Bejczy, "Teleoperator/robot technology can help solve biomedical problems," Jet Propulsion Laboratory, Pasadena, CA, Tech. Memo. 33-271, Jan. 1, 1975.

[21] S. Charles, R. E. Williams, and B. Hamel, "Design of a surgeon–machine interface for teleoperated microsurgery," in *Proc. Int. Conf. IEEE Engineering in Medicine and Biology Society*, vol. 11, 1989, pp. 883–884.

[22] J. A. McEwen, C. R. Bussani, G. F. Auchinlech, and M. J. Breault, "Development and initial clinical evaluation of pre-robotic and robotic surgical retraction system," in *Proc. Int. Conf. IEEE Engineering in Medicine and Biology Society*, vol. 11, 1989, pp. 881–882.

[23] A. Sabatini, M. Bergamasco, and P. Dario, "Force feedback-based telemicromanipulation for robot surgery in soft tissues," in *Proc. Int. Conf. IEEE Engineering in Medicine and Biology Society*, 1989, vol. 11, pp. 890–891.

[24] B. Davies, R. D. Hibberd, W. S. Ng, A. G. Timoney, and J. E. A. Wickham, "A robotic assistant for prostate surgery," in *Proc. Int. Conf. IEEE Engineering in Medicine and Biology Society*, 1992, vol. 14, p. 1052.

[25] J. W. Hill, P. S. Green, J. F. Jensen, Y. Gorfu, and A. S. Shah, "Telepresence surgery demonstration system," in *Proceedings 1994 IEEE International Conference on Robotics and Automation*. San Diego, CA: IEEE Robotics Autom. Soc., May 8–13, 1994, vol. 3, pp. 2302–2307.

[26] F. Tendick, S. S. Sastry, R. S. Fearing, and M. Cohn, "Applications of micromechatronics in minimal invasive surgery," *IEEE Trans. Mechatronics*, vol. 3, no. 1, pp. 34–42, Mar. 1998.

[27] A. Bicchi *et al.*, "A sensorized minimally invasive surgery tool for detecting tissue elastic properties," in *Proc. 1996 IEEE Int. Conf. Robotics and Automation*, Minneapolis, MN, Apr. 1996, pp. 884–888.

[28] A. Morimoto *et al.*, "Force sensor for laparoscopic babcock," *Stud. Health Technol. Inform.*, vol. 39, pp. 355–361, 1997.

[29] L. R. Rabiner, "A tutorial on hidden Markov models and selected application in speech recognition," *Proc. IEEE*, vol. 77, Feb. 1989.

[30] H. Frank and S. C. Althoen, *Statistics—Concepts and Application*. Cambridge, U.K.: Cambridge Univ. Press, 1994.

[31] *System Identification Toolbox User's Guide (For use with Matlab)*, MathWorks, Natick, MA, 1998.

[32] J. K. Baker, "The DRAGON system—An overview," *IEEE Trans. Acoust. Speech Signal Processing*, vol. ASSP–23, pp. 24–29, Jan 1975.

[33] S. E. Levinson, L. R. Rabiner, and M. M. Sondhi, "An introduction to the application of the theory of probabalistic functions of a Markov process to automatic speech recognition," *Bell Sys. Tech. J.*, vol. 62, no. 4, pp. 1035–1074, 1983.

[34] R. Reddy, "Foundations and grand challenges of artificial intelligence: 1988 AAAI presidential address," *AI Mag.*, pp. 9–21, Winter 1988.

[35] B. Hannaford and P. Lee, "Hidden Markov model analysis of force/torque information in telemanipulation," presented at the 1st Int. Symp. Experimental Robotics, Montreal, Canada, June 1989.

[36] ——, "Hidden Markov model of force torque information in telemanipulation," *Int. J.Robot. Res.*, vol. 10, no. 5, pp. 528–539, 1991.

[37] ——, "Multi-dimensional hidden Markov model of telemanipulation tasks with varying outcomes," presented at the IEEE Int. Conf. Systems Man and Cybernetics, Los Angeles, CA, Nov. 1990.
[38] P. Pook and D. H. Ballard, "Recognizing teleoperated manipulations," in *Proc. IEEE Robot. Automat.*, vol. 2, Atlanta, GA, May 1993, pp. 578–585.
[39] M. C. Nechyba and Y. Xu, "Stochastic similarity for validating human control strategy models," *IEEE Trans. Robot. Automat.*, vol. 14, pp. 437–451, June 1998.
[40] Y. Jie, X. Yangsheng, and C.-S. Chen, "Human action learning via hidden Markov model," *IEEE Trans. Syst. Man Cybern. A*, vol. 27, pp. 34–44, Jan. 1997.
[41] K. Itabashi, K. Hirana, T. Suzuki, S. Okuma, and F. Fujiwara, "Modeling and realization of the peg-in-hole task based on hidden Markov model," in *Proc. IEEE Int. Conf. on Robotics and Automation*, Leuven, Belgium, May 1998, p. 1142.
[42] B. Hannaford, "Hidden Markov model analysis of manufacturing process information," presented at the IROS 1991, Osaka, Japan, Nov. 1991.
[43] B. J. McCarragher, G. Hovland, P. Sikka, P. Aigner, and D. Austin, "Hybrid dynamic modeling and control of constrained manipulation systems," *IEEE Robot. Automat. Mag.*, vol. 4, June 1997.
[44] I. Wachsmuth and M. Frohlich, Eds., *Gesture and Sign Language in Human–Computer Interaction, International Gesture Workshop Proceedings*. Berlin, Germany: Springer-Verlag, 1998, p. xi+308.
[45] J.-J. Lien, T. Kanade, J.-F. Cohn, and C.-L. Ching, "Automated facial expression recognition based on FACS action units," in *Proc. 3rd IEEE Int. Conf. Automatic Face and Gesture Recognition*, Nara, Japan, April 14–16, 1998, Cat. no. 98EX107, pp. 390–395.
[46] P. Baldi and S. Brunak, *Bioinformatics*. Cambridge, MA: MIT Press, 1998.
[47] K. Kwon, "Application of HMM to accident diagnosis in nuclear power plants," in *Proc. Topical Meeting Computer-Based Human Support Systems*. Phil., PA: Amer. Nuclear Soc., June 1995.
[48] P. Freed, "Detecting pulsars with hidden Markov models," in *Proc. 3rd Int. Symp. Signal Processing and Applications*, vol. 1, Aug. 1992, pp. 179–183.

Jacob Rosen received the B.Sc. degree in mechanical engineering, and the M.Sc. and Ph.D. degrees in biomedical engineering from Tel-Aviv University, Tel-Aviv, Israel, in 1987, 1993, and 1997 respectively.

From 1987 to 1992, he served as Officer in the IDF studying human–machine interfaces. From 1993 to 1997, he was a Research Associate developing and studying the electromyogram-based powered Exoskeleton at the Biomechanics Laboratory, Department of Biomedical Engineering, Tel-Aviv University. During the same period of time, he held a biomechanical engineering position in a startup company developing innovative othopedic spine/pelvis implants. Since 1997, he has been at the University of Washington, Seattle, where he has been Research Assistant Professor of Electrical Engineering since 2000. His research interests focus on biomechanics, biorobotics, and human–machine interface.

Blake Hannaford (S'82–M'84) received the B.S. degree in engineering and applied science from Yale University, New Haven, CT, in 1988, and the M.S. and Ph.D. degrees in electrical engineering from the University of California, Berkeley, in 1982 and 1985, respectively. At Berkeley, he pursued thesis research in multiple target tracking in medical images and the control of time-optimal voluntary human movement.

Before graduate study, he held engineering positions in digital hardware and software design, office automation, and medical image processing. From 1986 to 1989, he worked on the remote control of robot manipulators in the Man–Machine Systems Group in the Automated Systems Section of the NASA Jet Propulsion Laboratory at the California Institute of Technology (Caltech), Pasadena. He supervised that group form 1988 to 1989. Since September 1989, he has been at the University of Washington, Seattle, where he has been Professor of Electrical Engineering since 1997. His currently active interests include haptic displays on the internet, surgical biomechanics, and biologically based design of robot manipulators. His lab URL is http://rcs.ee.washington.edu/BRL.

Dr. Hannaford was awarded the National Science Foundation's Presidential Young Investigator Award and the Early Career Achievement Award from the IEEE Engineering in Medicine and Biology Society.

Christina G. Richards completed medical school at the Ohio State University, Columbus. She completed a residency in general surgery at the Medical College of Wisconsin, Milwaukee, followed by a fellowship in laparoscopic surgery at the University of Washington, Seattle.

She is currently in private practice in Salt Lake City, UT.

Dr. Richards is a member of the American College of Surgeons, Society for Surgery of the Alimentary Tract and Society of American Gastrointestinal and Endoscopic Surgery.

Mika N. Sinanan received the M.D. degree from Johns Hopkins University, Baltimore, MD, in 1980 and the Ph.D. degree in gastrointestinal physiology from the University of British Columbia, Vancouver, Canada, in 1991. He completed training in general and gastrointestinal surgery at the University of Washington (UW), Seattle, in 1988.

He joined the faculty to UW in 1988. Currently, he is an Associate Professor of Surgery and Adjunct Associate Professor of Electrical Engineering at UW. His research interests focus on technical surgical education, clinical application of advance videoendoscopic surgical procedures, and the study of force application and development of new instruments for technical maneuvers in minimally invasive surgery.

Dr. Sinanan is a member of the American College of Surgeons, Society for Surgery of the Alimentary Tract, Society of American Gastrointestinal and Endoscopic Surgeons, and other regional societies.